# Seismic Response of offshore wind turbine foundations

**R.S. Kourkoulis & F.M. Gelagoti**
*Soil Mechanics Laboratory, NTUA, Greece*

**A.M. Kaynia**
*Norwegian Geotechnical Institute, Oslo, Norway*

**SUMMARY:**
This paper investigates the response of wind turbines founded on suction caissons with due account of non-linear soil-structure interaction. The models are subjected to static cyclic and earthquake loading in order to parametrically explore the role of potential non-linear interface behavior materialized through sliding between the caisson skirt and the soil or gap formation. It is shown that interface failure may substantially reduce the capacity of such foundations, while the effect becomes more intense as the caisson depth decreases. When subjected to earthquake shaking, imperfect interface conditions may limit the tower bending but produces irrecoverable displacement on the nacelle level; a direct result of the accumulated rotation at the foundation. This undesirable rotation may be more effectively prevented by increasing the caisson diameter rather than its depth of embedment.

*Keywords: Suction caissons, earthquake, non-linear interface properties*

## 1. INTRODUCTION - SCOPE OF STUDY

Installation of off-shore wind-farms of significant turbine capacities is planned with increasing frequency worldwide as a result of the consistently high winds in such environments which guarantees reliable high power output. The operation of a wind turbine generates substantial horizontal loading which may be of the order of 65% of the vertical load in relatively lightweight systems. (*Houlsby & Byrne, 2000*). Thus, the foundation design must ensure safety against large overturning moments under comparatively low vertical loading. Among a variety of foundation schemes that have been proposed and utilized so far, suction caissons are nowadays increasingly popular as they ease the installation process and are able to safely carry significant overturning moments (*Byrne, 2000; Houlsby et al, 2005*). Although a decent amount of research has been carried out regarding the behavior of wind turbines under static and monotonic loading, little research data are available considering their response under earthquake loading. The latter is expected to act simultaneously with wind loading and could significantly increase the overturning moment transmitted to the foundation.

The present paper investigates the response of wind turbines founded on suction caisson taking account of soil-structure interaction by means of non-linear numerical analyses. Great emphasis is placed on exploring the role of potential non-linear interface behavior materialized either through detachment and sliding between the caisson skirt and the soil, or through uplifting of the caisson lid from the underlying soil due to insufficient suction, when subjecting the models to either static cyclic or earthquake loading.

## 2. PROBLEM DESCRIPTION AND NUMERICAL MODELING

The problem under study refers to a typical offshore wind turbine founded in a homogeneous clay stratum with $S_u$ = 60 kPa and $E_{stat}$ = 30 MPa through a suction caisson (Fig. 1a). The caisson diameter has been taken equal to 20 m, which could be considered representative foundation for a 3.5 MW turbine or a conservative design for a 2MW turbine. The dimensions and design loads of such systems are displayed in Table 1. The cases examined in the ensuing compare the response of a shallow caisson with embedment-diameter ratio (D/B) equal to 0.2 with that of a deeply embedded alternative with D/B = 0.5.

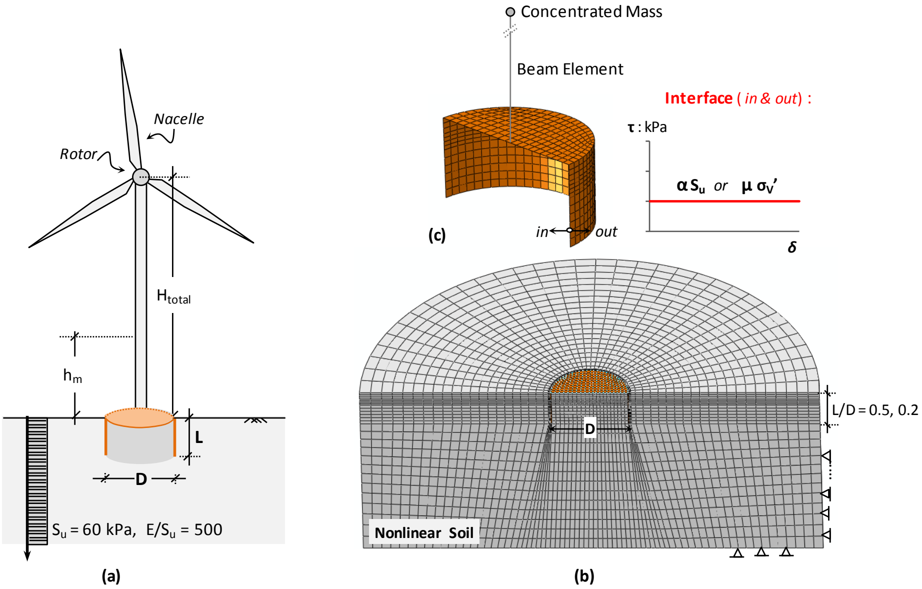


**Figure 1. (a)** Simplified geometry of the system under study; **(b)** A view of the 3-dimensional FE model and **(c)** Modeling details: the caisson is modeled with shell elements, while the interface between the caisson and the surrounding-encased soil is simulated with contact elements that allow slippage and/or detachment.

**Table 1.** Geometrical Characteristics and Foundation loads adopted in the examples

| Wind-turbine capacity | $H_{total}$ : m | $m_{total}$ : tn | $M_{design}$ : MNm | $H_{design}$ : MN |
|---|---|---|---|---|
| **2 MW** | 60-70 | 250 - 350 | 70 - 90 | 2-3 |
| **3.5 MW** | 90-100 | 500 - 600 | 100 - 130 | 4-5 |

The problem is analyzed through 3-D finite element (FE) analysis accounting for material and geometric nonlinearities. The developed 3D FE model, taking advantage of symmetry due to the problem geometry, is displayed in Figure 1b. 8-noded hexahedral continuum elements have been used for soil modeling whose nonlinear behavior is modeled through a simple kinematic hardening model with Von Mises failure criterion, and associated flow rule that is considered appropriate for clay under undrained conditions (*Anastasopoulos et al. 2012*). The soil–caisson interface is modeled using special contact elements. The properties of the latter can be appropriately adjusted so as to simulate either *perfect interface conditions* (where the full shear strength of the model may be mobilized and full tensile strength can be developed), or *imperfect interface conditions* (where reduced shear strength is mobilized and detachment between the soil and the foundation is possible). In this second case, the maximum interface strength has been calculated as a function of either : (a) the coherence of the soil surrounding the caisson skirt [expressed as a ratio *a* of the soil strength $S_u$] or (b) the friction developed on the skirt-soil interface [expressed through the friction coefficient $\mu$ (Fig. 1c)].

## 3. FAILURE ENVELOPES ASSUMING FULLY BONDED INTERFACE CONDITIONS

### 3.1 Tests Description and Validation

The initial series of analyses refer to the case of perfect interface conditions which is the most common case for off-shore foundations (e.g. *Gourvenec 2007; Yun & Bransby, 2007*). The role of these analyses is twofold as they serve both as validation of the numerical methodology and as a means to investigate the effect of the depth of embedment under fully 3–dimensional conditions. The first part is achieved through comparison of the numerical prediction with published results for the case of a surface foundation, while the second through the comparative examination of the response of the lightly and the deeply embedded foundation.

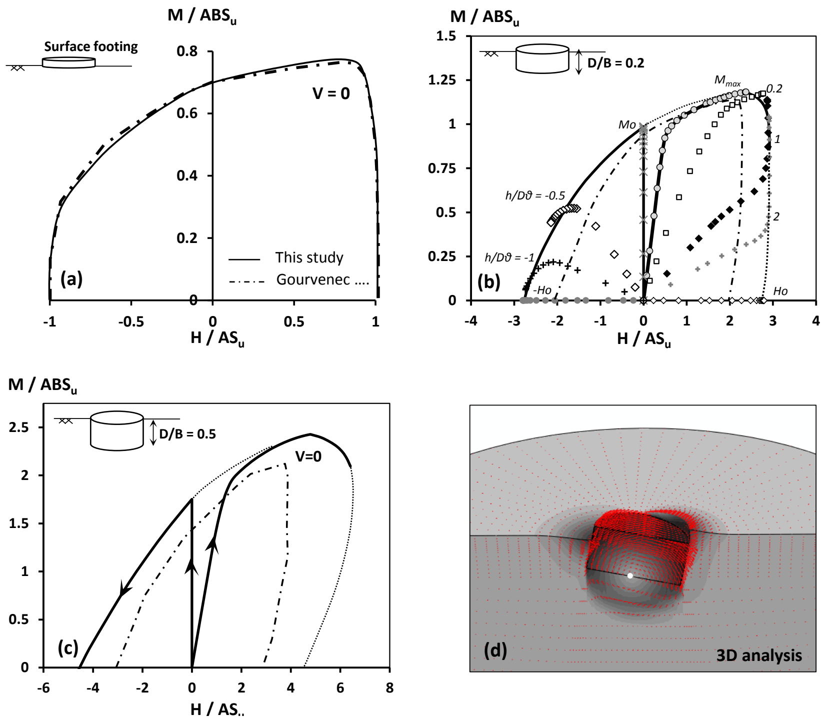


**Figure 2.** Produced failure envelopes in the H-M space and comparison with plane strain results by *Gourvenec (2008)* assuming fully bonded interface conditions for **(a)** surface foundation and for a caisson with embedment ratio **(b)** D/B =0 and **(c)** D/B = 0.2 **(d)** Deformed mesh sketch explaining the difference between 2D and 3D analysis .

In all these cases, results are presented in terms of failure envelopes in the M-H (moment – horizontal loading) space under conditions of zero vertical load. In order to define the failure envelope, both constant–ratio displacement probe tests and displacement controlled swipe tests were carried out. Displacements were in all cases applied on the central node of the foundation base.

Swipe tests (*Tan, 1990*) are useful method to produce the failure envelopes as they allow the generation of the complete failure envelope through one single analysis. However, they should be treated with caution especially in the case of the M-H space (*Gourvenec & Randolph, 2003*) as they may intersect the true failure envelope. On the other hand, probe tests for the case of a footing of diameter B, consist of the application of constant ratio combinations ($v/B\vartheta$ = const or $h/B\vartheta$ = const) of rotation ($\vartheta$) and vertical or horizontal displacement (v or h). These produce load paths which commence from the origin, and evolve until reaching the failure envelope along which they travel afterwards. The termination points of a set of probe tests at various displacement ratios will ultimately define the failure envelope.

### 3.2 Results

Following the commonly applied practice, results are presented in dimensionless form ($M/ABS_u$ , $H/AS_u$) where A the foundation area. A remarkable agreement may be observed between these results and those published by *Gourvenec (2007)* for the case of the surface foundation (Fig. 2a). Increasing the depth of embedment leads to a substantial increase of the foundation capacity both in pure horizontal, or moment loading and in combinations thereof (Figs 2b and c). The asymmetry of the M-

H diagram observed by *Ukritchon et al. (1998), Yun & Bransby (2007) and Gourvenec and Randolph (2003),* is once more confirmed. However, the calculated failure envelopes seem to be even more expanded than those produced by plane strain analyses, while the discrepancies become more intense as the embedment depth increases. This phenomenon is mainly due to the three-dimensional problem geometry (Fig. 2d): apart from the mobilization of the active and passive soil resistance in the front and rear faces of the foundation, 3D analysis captures the mobilization of lateral shear resistance of the soil which, understandably, becomes even more prominent as the area of the lateral faces (i.e. the depth of embedment) increases.

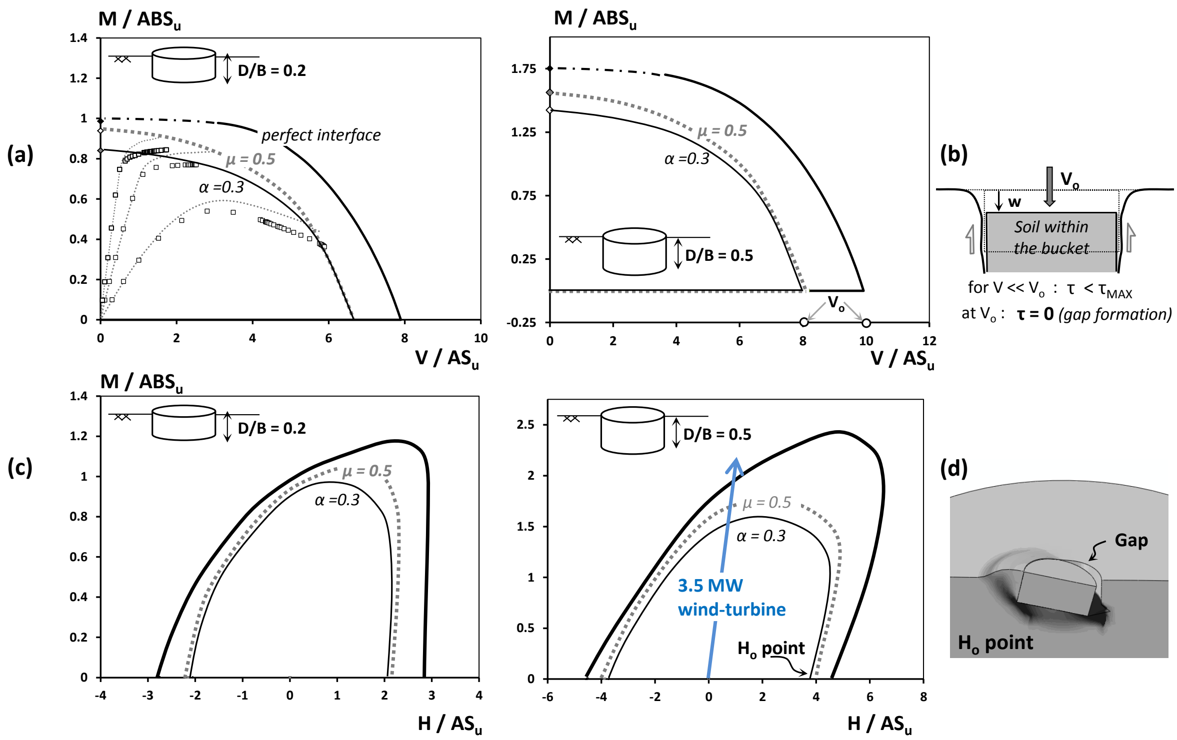


**Figure 3.** Effect of external interface conditions on the H-M and V-M failure envelopes of a caisson with embedment ratio D/B = 0.2 and D/B = 0.5. **(a)** V-M failure envelopes , **(b)** Schematic explanation of the procedure of gap formation between the foundation and the soil during push-down loading, **(c)** H-M failure envelopes and **(d)** deformed mesh under pure horizontal loading.

## 4. ALLOWING SEPARATION OF THE SUCTION CAISSON FROM SURROUNDING SOIL

As implied by the previous discussion, the full shear strength between the caisson and the soil may not always be available as a result of either gradual soil degradation during cyclic loading or a number of factors related to the installation process. For example, the potential plastic straining along the interface during driving of the skirt would limit the shear strength that may actually be developed. As it is impossible to estimate the actual interface strength a priori, its effect is herein investigated parametrically. In an attempt to isolate the effect of each interface, it is at this stage assumed that the caisson lid maintains perfect contact with the underlying soil (i.e. full suction is achieved) and that the same holds true between the caisson skirt and internal soil. Results are presented for the two example foundations investigated previously adopting the following assumptions for the interface conditions between the caisson skirt and the surrounding soil :

(i) the interface strength is determined by a friction coefficient of **μ** = 0.5

(ii) the strength along the interface is assumed to be a fraction (***a***) of the undrained shear strength of the soil. Based on centrifuge data by *Gourvenec et al. (2009)* factor *a* has been assumed equal to 0.3.

Results are plotted in terms of V–M (H = 0) and H–M (V = 0) failure envelopes (Fig. 3). The existence of the interface in general reduces the foundation capacity for all types of loading and embedment ratios. However, disparities between the two distinct interface conditions are much less pronounced regardless of the D/B ratio. Observe for example that in the case of V–M loading (Fig. 3a) both curves originate at exactly the same value of maximum vertical load $V_{o,}$ while they tend to slightly deviate as the locus approaches $M_o$ (which is of course reduced compared to the full-contact case). The explanation of this behavior is offered schematically by Fig.3b: the downwards translation of the foundation initiates the formation of a gap between the skirt and the soil which keeps expanding along the interface until ultimately, contact has totally vanished. Hence the measured bearing capacity will only be attributable to the base ("tip") resistance of the caisson which is apparently only a function of the embedment depth and utterly independent of the lateral interface strength.

In the M-H space (Fig. 3c) the existence of the interfaces not only shrinks but also tends to smoothen the failure loci causing them to deviate from their usual non-symmetric shape. The disparities are more pronounced for the D/B = 0.5 foundation where the skirt area –and hence the effect of the lateral shear resistance on the total strength – is higher, resulting to a decrease of the maximum moment of about 60%. Again, differences between the two interface conditions are not that evident, while they are almost negligible at point of pure horizontal load $H_o$. Observe (Fig. 3d) that at the instant of attainment of $H_o$, foundation-soil contact has practically ceased to exist along a substantial area of the skirt. Therefore, differences between the two cases are only due to the shear developed along this limited part of the skirt that still maintains contact with the soil.

## 5. ACCOUNTING FOR POSSIBLE SEPARATION OF SUCTION CAISSON FROM ENCASED AND SURROUNDING SOIL

The previous sections typically refer to off-shore wind turbine foundations. However, results are readily applicable to any type of embedded foundation which may be either in contact or able to detach from the surrounding soil. The very nature of suction caissons however may also allow detachment between the caisson skirt and the soil both internally and externally as well as between the caisson lid and the underlying soil. Although questionable, this study will assume constant contact between the lid and the soil thus neglecting the effect of their possible separation.

Conventional failure envelopes (as those presented so far) are obviously inappropriate to capture such phenomena as they are produced by application of displacement on their base; thus they intrinsically ignore the potential interaction between the steel caisson and the soil. Yet, loading from wind turbines (stemming either from earthquake or simply from the wind, sea waves or currents) is transmitted from the turbine tower to the caisson top and, separation of the latter from the soil may modify the amount of loading conveyed to its base.

Therefore, the analyses presented in this section refer to displacement-controlled loading applied at the center of mass of the 3.5MW turbine described in Figure 1. An initial set of analyses are conducted in order to obtain the monotonic moment – rotation curve. Then, the wind turbine models are subjected to cyclic loading consisting of three cycles of applied displacement of constant amplitude as explained in the sequel. Understandably, the latter analyses do not aim at capturing the effects of fatigue (due to numerous cycles of wind loading) but rather attempt a preliminary manifestation of the possible impact of earthquake loading in a simplified manner. Results are offered in terms of moment-rotation curves calculated on the base of the tower (ie foundation top) and represent the actual moment demand on the foundation.

### 5.1 Response under Monotonic Loading

Figure 4 compares the *M-θ* curves generated during monotonic loading of the turbine for two cases of interface conditions:

(i) Detachment permitted only along the external interface and
(ii) Detachment permitted both along the external and the internal interface

The interface strength is similarly to the previous case governed either by friction (displaying results for the extreme case of friction coefficient μ = 1) or by a coherence coefficient $\alpha = 0.3$ (i.e. $Su_{,res}$ = 20 kPa). As expected, the reduction of the shear resistance along the skirt results in reduction of both the stiffness and the ultimate capacity of the soil-foundation system. Observe that this reduction may be substantial compared to the perfect-interface assumption (thin solid line), revealing that design based on such an approach may well be un-conservative, especially when accounting for the extremely limited rotational tolerance requirements of wind turbine towers. Apart from that, in terms of foundation comparisons, it is worth mentioning that the high-friction assumption (μ=1) results in negligible differences between the two interface scenarios (only external *vs* external and internal) at least for deeply embedded foundation (Fig. 4a). This phenomenon owes to the fact that the combination of the adequate skirt area of the D/B = 0.5 caisson with such a level of μ, results in a significant friction force which impedes detachment of the skirt from the internal soil. On the contrary, when the skirt area is lower as in the D/B = 0.2 scenario (Fig. 4b), the substantially lower friction force becomes critical and the skirt manages to slide along the internal soil interface. Evidently, when the interface strength reduces even more to $0.3S_u$ sliding becomes the prevailing mechanism even for the high D/B ratio.

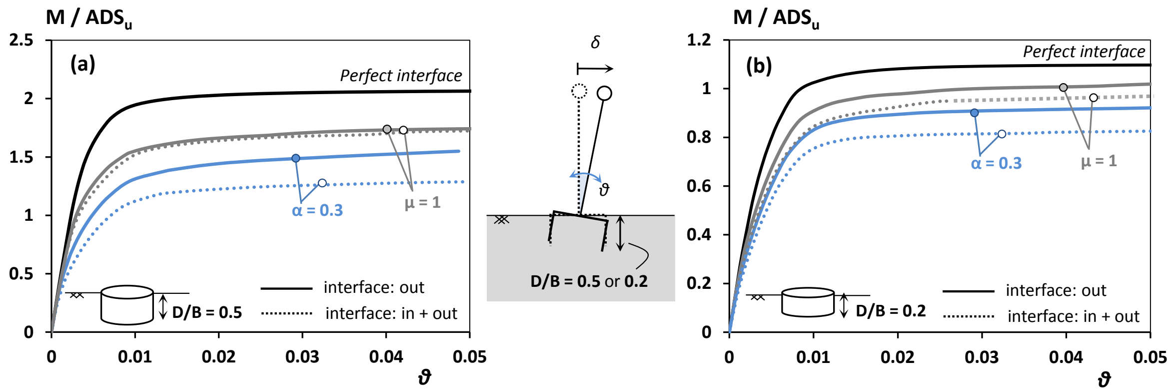


**Figure 4.** Effect of interface properties between the suction caisson and the soil: Moment-Rotation curves produced during monotonic horizontal loading of a 3.5 MW wind turbine assuming a suction caisson of embedment **(a)** D/B=0.5 and **(b)** D/B=0.2.

## 5.2 Response under Cyclic Loading

Under cyclic loading the possibility of soil-caisson detachment may completely modify the expected response. This is clearly illustrated in Fig. 5 where the deeply embedded foundation is imposed to both low and high amplitude slow cyclic push-over loading. As long as the applied displacement is maintained low enough, practically within the elastic range of response (θ = 0.01 rad) the shape of the produced loops is not affected by the interface conditions as no separation between the caisson and the soil tends to take place (gray line in Figs. 5a and b). The difference is more conspicuous for the higher amplitude rotation of θ = 0.05 when the shape of the loop past the first cycle tends to deviate from the monotonic curve. This characteristic pinched shape is the outcome of the creation of an irrecoverable gap behind the foundation: as the caisson rotates during the first cycle towards one direction, it produces plastic deformation of the reacting soil (Fig. 5c), which is apparently not recovered once the direction of loading is reversed. Consequently, during the second cycle of loading towards the same direction, soil resistance is reduced due to the existence of the gap which is in turn is reflected on the modified shape of the loop.

Further reduction of the interface strength results in reduced overall system strength which causes the loop area to shrink preserving however its aforementioned characteristic pinched shape (Fig 6a). Interestingly though, in the case of the low D/B ratio (Fig 6b), even for the weakest interface scenario, the shape of the M-θ loop is apparently more rounded: the foundation response is controlled by the mobilized strength at the caisson base, while the lateral resistance and thus the possible formation of a gap cannot substantially modify the response among sequential cycles of loading (Fig 6b). It is worth mentioning that, although the above findings once more reveal that the assumption of perfect interface conditions between the soil and the caisson should be treated with caution as it may lead to grossly un-conservative estimates in design, the examined cases are extreme and at this stage they only aim to highlight the potential effects rather than accurately quantify them.

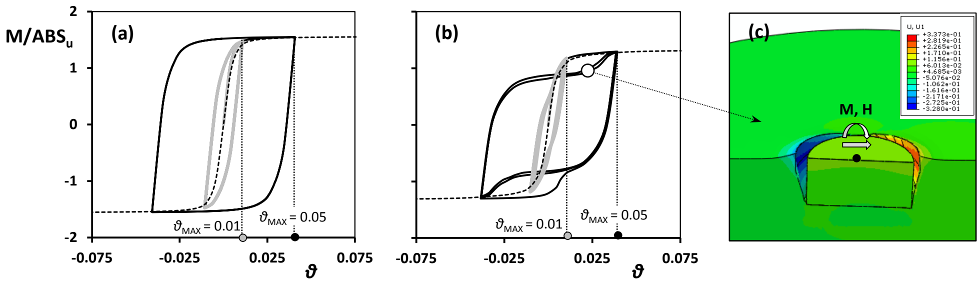


**Figure 5.** Low-amplitude (gray line) high amplitude (black line) M-θ loops produced during horizontal slow-cyclic loading of the wind turbine on a **D/B = 0.5** suction caisson assuming **(a)** full contact conditions between the caisson and the soil and (b) allowing the foundation to detach from the surrounding soil. **(c)** Displacement contours explaining the pinching shape of the M-θ loop.

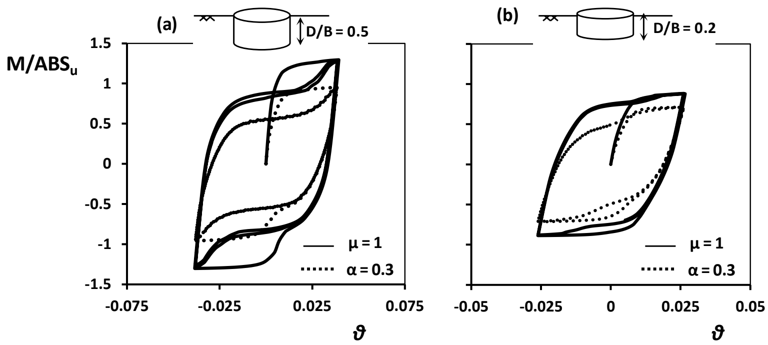


**Figure 6.** Effect of the external interface properties on the M-θ loop produced during cyclic loading of a turbine founded on a suction caisson with embedment (a) D/B = 0.5 and (b) D/B= 0.2

## 6. SEISMIC LOADING OF WIND TURBINE

Having identified the possible impacts of non-linear interface behavior under monotonic or cyclic loading, this section attempts a preliminary assessment of its potential impacts when the simplified turbine model is subjected to earthquake loading. Proper kinematic constraints have been assumed at the lateral boundaries of the FE model to simulate free-field response, while dashpots elements have been used at the base of the model to correctly reproduce radiation damping. The earthquake motion is applied at the base nodes so as to allow for correct representation of kinematic soil-foundation interaction effects. Two earthquake scenarios have been examined: (a) the Takatori (Kobe, 1995) and (b) the Rinaldi (Northridge, 1994) records. The results presented in this section refer to a 2 MW wind turbine (with its characteristics described in Table 1). Following the same rationale as previously, we first study the response of a shallow caisson foundation of B=16m and D/B =0.2 m comparing the two extreme interface conditions: perfect interface against the fully non linear case characterized by reduced soil-skirt interface strength of 0.3$S_u$.

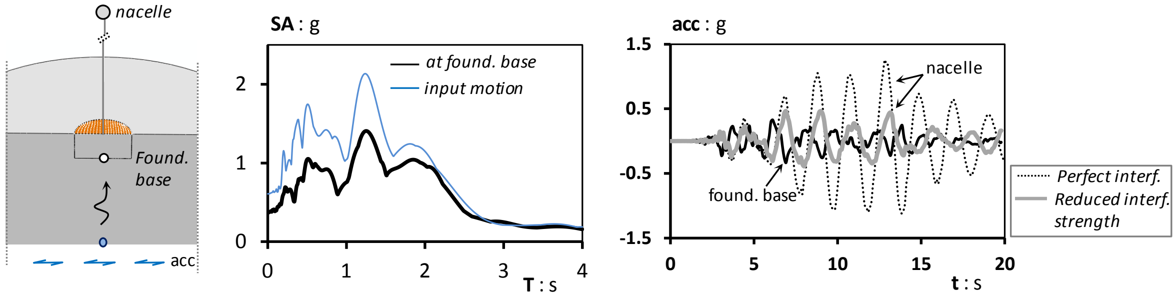


**Figure 7.** Wind turbine subjected to the *Takatori* record : **(a)** Response spectra of the input motion and the computed motion at the foundation base; **(b)** acceleration time histories at the foundation (black line) and at the nacelle level assuming perfect interface (dotted line) and imperfect interface conditions (gray line).

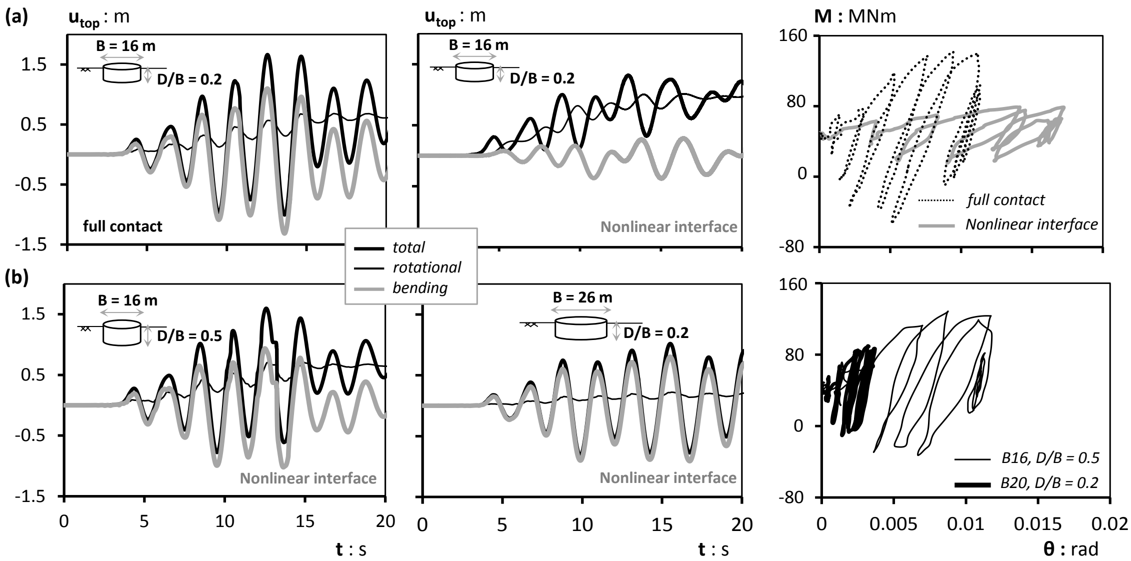


**Figure 8.** Displacement time histories at the nacelle level and Moment rotation plots at foundation level for a 2MW wind turbine subjected to the *Takatori* record for all cases examined

In the first example the wind turbine is excited at its base (i.e. at -40 m) by the Takatori record. This accelerogram is characterized by a multitude of strong motion cycles and a quite long duration. Application of such a severe record on the base of a Su = 60 kPa soil profile is expectedly followed by significant plastic straining of the soil which consequently modifies the motion experienced by the turbine both in terms of amplitude and characteristics (Fig 7). Still however, the response spectrum calculated at the foundation base level demonstrates apparently high values within a period range of $0.8 < T < 2.2$ s. Figure 7b plots the acceleration time histories at the foundation tip along with the time histories recorded at the nacelle level for the two interface scenarios examined.

Figures 8a and b compare the performance of the two interface scenarios in terms of displacement time histories produced on top of the turbine at the nacelle level (plots are truncated at t=20s). Evidently, despite the intensity of the ground shaking, in case of full contact, the foundation performs quite satisfactorily ensuring practically negligible rotation. Displacement on the tower top is largely due to tower bending (i.e. may be reduced in case of a stiffer tower) and despite the fact that its peak value exceeds 1.5 m, it is almost totally recoverable afterwards. On the other hand, interface failure produces quite ambivalent consequences as it does result in significantly reduced stressing of the tower but augments the displacement experienced at the nacelle level both in terms of peak as well as residual value. Indeed, as evidenced by Fig. 8b, displacement due to tower bending is now quite insignificant reaching a mere 25cm; a substantial improvement compared to the almost 1.4m of the previous case. This is the consequence of interface failure which allows the caisson to rotate (Fig. 8c) thereby limiting the inertial loading transmitted onto the superstructure. Yet, the rotation-induced total displacement, which in terms of amplitude remains almost unchanged, keeps accumulating throughout the time history. This displacement is irrecoverable after the end of shaking which raises serious concerns about the serviceability of the turbine.

Improving the foundation performance would entail either an increase of the skirt length (i.e. D/B ratio) or a diameter increase while maintaining the D/B ratio constant as outlined in Figures 9 d-f, which compare the response of a B=16m caisson with D/B = 0.5 with that of a B = 20 m caisson with D/B = 0.2. Apparently, performance is in both cases substantially improved in terms of foundation rotation (and hence residual displacement). Surprisingly however, despite its noteworthy depth increase, the D/B = 0.5 caisson does not demonstrate such a competent performance as the B = 20 m alternative. The latter practically wipes out the foundation rotation while simultaneously reduces the distress of the superstructure (Fig. 8e)

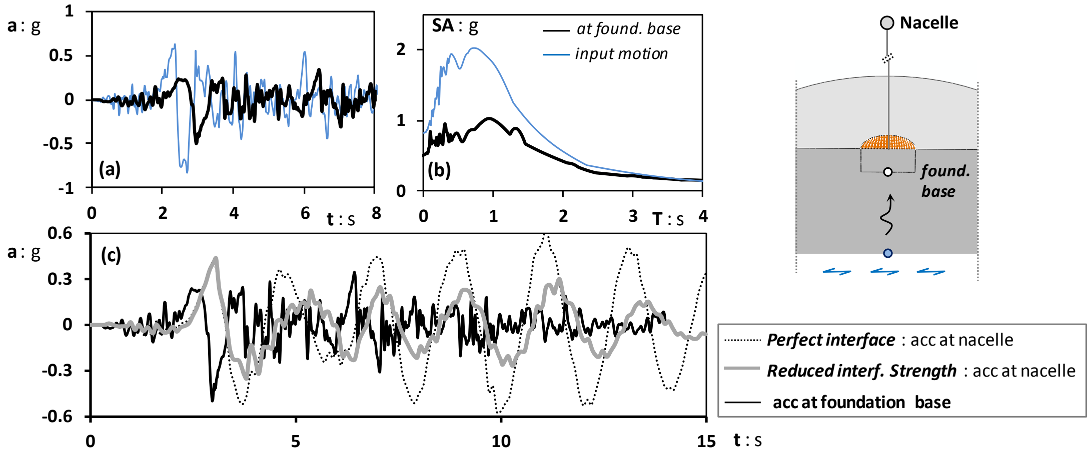


**Figure 9.** Wind turbine subjected to the *Rinaldi* record : **(a, b)** Acceleration time histories and response spectra of the input (blue line) and the computed motion at the foundation base (black line). **(c)** Acceleration time histories at the foundation (black line) and the nacelle level assuming perfect (dotted line) and imperfect interface conditions (gray line).

In the second example the turbine is excited by the Rinaldi record. The original record has a much lower duration than the previous one, yet its effect is engraved by its striking long-duration single pulse of 0.82g (Fig 9a). The severity of the pulse produces substantial soil plastification as the seismic waves propagate towards the model surface therefore leading to a conspicuous de-amplification of the excitation ultimately experienced at the foundation base. Figure 9c, plots the acceleration time histories on the turbine (top) for the two extreme interface scenarios. In terms of loading transmitted to the superstructure, this result is reminiscent of the previously discussed phenomena: perfect interface prevents foundation detachment from the soil and allow the full earthquake loading to be transmitted to the turbine. On the other hand, sliding at the skirt-soil interface reduces the acceleration on the turbine but necessitates significant foundation displacements, which are eventually conveyed to the superstructure (Fig. 10). The bending drift is indeed reduced; its residual value drops almost to 0— yet the total residual drift of the turbine corresponds to a 0.5 m displacement at its top; a value that may question its serviceability (Fig. 10b). It is worth mentioning that for these particular low interface strength assumptions, the foundation moment demand exceeds its capacity as exhibited by the formation of a clear plateau at around 80 MNm in the M-θ loop (Fig. 10c). It is concluded that although the assumptions adopted herein correspond to a quite conservative strength scenario they must be regarded as indicative of the potential importance of interface details.

## 7. CONCLUSIONS

This paper has investigated the role of potential non-linear interface behavior on the seismic response of wind turbines founded on suction caissons subjected to both extreme and moderate loading scenarios. Although not exhaustive, this parametric analysis has highlighted a number of very interesting issues summarized below. It has been shown that reduced interface properties between the caisson and the soil (i.e. reduced soil shear strength and tensionless interface) limit the foundation vertical capacity, while, in the M-H space tend to shrink the failure loci causing them to deviate from their usual non-symmetric shape. Cyclic loading loops may in that case demonstrate a characteristic pinched shape reminiscent of that produced during rocking of shallow footings. Furthermore, when considering imperfect interface conditions, the depth of embedment becomes critical as it defines the amount of shear force that may be developed. When subjected to earthquake shaking, the imperfect interface permits skirt detachment from the soil which, combined with sliding at the soil-skirt interface may enable foundation rotation. The latter limits the tower bending but produces irrecoverable displacement on the nacelle level. Our limited sensitivity analysis has revealed that such a rotation may be more effectively prevented by increasing the caisson diameter rather than its depth of embedment.

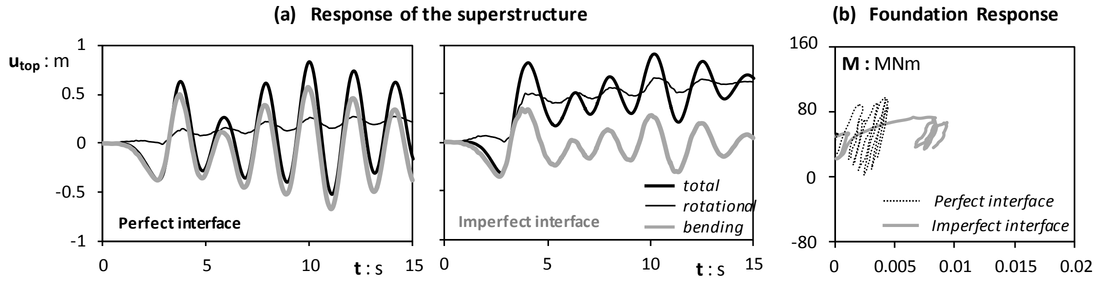


**Figure 10.** Seismic response of a 2MW wind turbine founded on a suction caisson of B=16 m and D/B=0.2 subjected to the *Rinaldi* record: (a) Displacement time histories at the nacelle level and **(b)** moment-rotation loops at the foundation. Perfect and imperfect interface conditions ($S_{u,res}$ = 20 kPa ) have been assumed.


**AKCNOWLEDGEMENT**

The first two authors were partially supported by the EU 7th Framework research project "Ideas" Programme, in Support of Frontier Research – Advanced Grant. Contract number ERC-2008-AdG 228254-DARE which is funded through the European Research Council (ERC)


**REFERENCES**


Anastasopoulos I., F. Gelagoti, R. Kourkoulis & G. Gazetas. 2011. Simplified Constitutive Model for Simulation of Cyclic Response of Shallow Foundations : Validation against Laboratory Tests. J. *Geotech. Geoenviron. Engng ASCE* **137: 12**, 1154–1168.

Byrne, B. W. 2000. Investigations of suction caissons in dense sand. ***DPhil thesis***. Univ. of Oxford, England.

Gourvenec, S. & Randolph, M. 2003. Effect of strength non-homogeneity on the shape and failure envelopes for combined loading of strip and circular foundations on clay. *Géotechnique* **53: 6**, 575–586.

Gourvenec, S. 2007. Failure envelopes of offshore shallow foundations under general loading. *Géotechnique* **57**

Gourvenec, S. 2008. Undrained bearing capacity of embedded footings under general loading. *Géotechnique* **58: 3**, 177–185

Gourvenec, S., Acosta-Martinex, E., and M. F. Randolph . 2009. Experimental study of uplift resistance of shallow skirted foundations in clay under transient and sustained concentric loading. *Géotechnique* **59: 6**

Houlsby, G.T. & Byrne, B.W. 2000. Suction Caisson Foundations for Offshore Wind Turbines and Anemometer Masts. *Wind Engineering* **24: 4**, 249-255

Houlsby, G.T., Ibsen, L-B. & Byrne, B.W. 2005. Suction caissons for wind turbines. *International Symposium on Frontiers in Offshore Geotechnics*, Perth, **Proceedings volume:** 75-94.

Tan, F.S. 1990. Centrifuge and Theoretical modeling of conical footings on sand. ***PhD Thesis***, Univ. of Cambridge, UK.

Ukritchon, B., Whittle, A. J. & Sloan, S. W. 1998. Undrained limit analysis for combined loading of strip footings on clay. J. *Geotech. Geoenviron. Engng ASCE* **124: 3**, 265–276.

Yun, G., & Bransby, M. 2007. The horizontal-moment capacity of embedded foundations in undrained soil. *Can Geotech. J.* **44:** 409-424